Original Article

Biophysical characterization of a model antibody drug conjugate

Tsutomu Arakawa[1],*, Yasunori Kurosawa[2], Michael Storms[2], Toshiaki Maruyama[2], C.J. Okumura[2], Nasib Karl Maluf[1]

[1] *Alliance Protein Laboratories, San Diego, CA, USA;*
[2] *Abwiz Bio, Inc., San Diego, CA, USA.*

Summary	Antibody drug conjugates (ADC) are important next-generation biopharmaceuticals and thus require stringent structure characterization as is the case for monoclonal antibodies. We have tested several biophysical techniques, *i.e.*, circular dichroism, analytical ultracentrifugation, differential scanning calorimetry and fluorescence spectroscopy, to characterize a fluorescein-labeled monoclonal antibody as a model ADC. These techniques indicated possible small structure and stability changes by the conjugation, while largely retaining the tertiary structure of the antibody, consistent with unaltered biological activities. Thus, the above biophysical techniques are effective at detecting changes in the structural properties of ADC.

Keywords: Circular dichroism, sedimentation velocity, calorimetry, antibody drug conjugate, biophysical characterization

1. Introduction

Targeted delivery of anti-cancer drugs and radioactive isotopes using cancer-specific antibodies, lipids and other compounds is currently being studied extensively as next generation biopharmaceuticals or diagnostic reagents (*1-8*). When antibodies and drugs are combined to make antibody-drug conjugates (ADC), also known as armed antibodies, the conjugation of what is often a hydrophobic drug to the antibody has the potential to alter the chemical and physical properties of the ADC. Pharmaceutical proteins, including antibodies, require extensive characterization of their structural properties, such as aggregation, conformation and stability (*9-12*). Such characterization is also required for ADC.

A number of biophysical techniques are used to characterize pharmaceutical proteins. Circular dichroism (CD) and Fourier-transform infrared spectroscopy (FTIR) are used to characterize protein conformation. Protein aggregation is commonly characterized by dynamic light scattering (DLS), static light scattering combined with size exclusion chromatography (SEC-MALS)

and analytical ultracentrifugation (AUC). Differential scanning calorimetry (DSC) is used to characterize the thermal stability of proteins. It would be of great interest to see if these techniques can be successfully applied to characterize ADCs, as the conjugated drugs may interfere with the optical and hydrodynamic properties of ADCs (*13*). Here, we have initiated a study on the biophysical characterization of a model ADC. For this model ADC, we have decided to use a fluorescent probe, fluorescein isothiocyntae (FITC), as an alternative compound to anti-cancer drugs. FITC has aromatic rings, similar to aromatic hydrophobic drugs and hence its conjugation with antibodies will likely challenge the structural features of the antibody in a manner similar to a conjugated drug. We have compared the intact (*i.e.* the non-labeled) and the FITC-labeled monoclonal antibody (mAb) using CD, fluorescence, DSC and AUC. Isoelectric focusing (IEF) was used to confirm FITC conjugation, which was also determined by UV and visible absorbance spectroscopy.

2. Materials and Methods

2.1. *Antibody preparation*

A rabbit IgG monoclonal antibody was generated against a phosphorylated peptide. Conditioned medium (CM) expressing the IgG in Chinese hamster ovary cells was subjected to Protein-A chromatography. After

loading the CM, the column was washed with 1 M arginine, 20 mM phosphate, pH 6.0 followed by elution of the bound IgG using Ajinomoto's Protein-A elution buffer (0.7 M arginine, 20 mM acetate, pH 4.1) (*14,15*). The eluted IgG solution was dialyzed against 10 mM sodium bicarbonate, pH 8.8.

2.2. FITC labeling

The above antibody solution (10 mL) was adjusted to 1 mg/mL protein. FITC (10-fold molar excess based on the molecular mass of 140,000 for the IgG) dissolved in 0.1 mL DMSO was added to the above antibody solution and incubated at room temperature for 15 hours. Unconjugated free FITC was removed by cation exchange Capto MMC mixed-mode chromatography in 20 mM phosphate at pH 6.5 and anion exchange Capto adhere mixed-mode chromatography in 50 mM Tris-HCl at pH 8.6. In both cases, FITC-labeled IgG bound to the column, while free negatively charged FITC flowed through the Capto MMC column. The bound FITC-IgG was eluted from the Capto MMC column with an arginine gradient from 0 to 1 M at pH 6.5 and from the Capto adhere column with an arginine gradient from 0 to 1.5 M at pH 8.6. The eluted FITC-IgG solution was dialyzed against 10 mM phosphate, pH 6.5. The intact protein was also dialyzed into the identical buffer.

2.3. CD spectroscopy

CD measurements were done using 0.416 mg/mL antibody solution (both FITC-IgG and intact IgG) in 10 mM phosphate, pH 6.5. Near and far UV CD spectra were determined at room temperature using a Jasco J-715 spectropolarimeter using 1 and 0.5 cm path-length cells. The spectra of free FITC were also determined using a solution of FITC that was equivalent to the concentration present in an FITC-IgG1 sample at 0.416 mg/mL. After subtracting the buffer spectrum, the CD spectra were converted to the mean residue ellipticity using the path-length of the cell, the protein concentration and the mean residue weight of 108 g/mol.

2.4. Isoelectric focusing

IEF experiments were done using 3-10 IEF gels, anode and cathode tank buffers, IEF sample buffer and IEF markers all from Life Technology. Electrophoresis was run by sequentially increasing the voltage from 100, 200 to 300 at 1 hour intervals. The gel was stained with Coomassie blue SimplyBlue SafeStain, also from Life Technology.

2.5. Analytical ultracentrifugation sedimentation velocity

Sedimentation velocity experiments were carried out using a Beckman XLI analytical ultracentrifuge. The parent IgG and FITC-IgG molecules were dialyzed against 10 mM phosphate, pH 6.5. The protein was diluted to 0.0.42 mg/mL using the dialysate and loaded (~450 μL) into 2-channel charcoal-epon centerpieces with a 12 mm optical pathlength using the dialysate as the reference solution. Data were collected at 280 nm, every 0.003 cm with no averaging in the continuous scan mode. The raw data were analyzed using the SEDFIT program (*16*) to obtain the sedimentation coefficient distribution.

2.6. Differential scanning calorimetry

The sample and reference cells of a TA Instruments Nano DSC were loaded using the autosampler with ~ 0.3 mL of sample and formulation buffer, respectively. The instrument was programmed to scan from 5 to 105°, at a rate of 60°C/hr, with a 5 second data averaging period. Several buffer *vs.* buffer scans were recorded throughout the experiment sequence to obtain a baseline scan to subtract from the experimental data and to ensure the sample and reference cells were adequately cleaned over the course of the experiment. Upon completion of a scan, the machine was programmed to clean the cells with a 5% Contrad solution, followed by an exhaustive water wash, and then the cells were reloaded with the next sample/buffer pair. The raw data were processed using NanoAnalyze version 3.1.2. A buffer-buffer scan was subtracted from each sample-buffer scan, and the baseline was calculated and processed using the NanoAnalyze software according to the manufacturer's instructions. The C_p profiles were normalized to protein concentration (expressed as kcal/mol/°C).

2.7. Fluorescence spectroscopy

The fluorescence emission spectra were collected using a Horriba Jobin Yvon FluoroMax-4 specrofluorometer. The excitation wavelength was set to 280 nm, and the emission spectra were collected at 90° from the excitation light source, from 295 to 500 nm, with an integration time of 0.2 s. The excitation and emission slits were set to 2 and 4 mm, respectively. The excitation and emission monochromators were calibrated according to the manufacturer's instructions using the water Raman peak. To obtain a true emission spectrum (*i.e.* independent of the instrument used to collect it), the spectra were corrected for instrument dependent factors according to the manufacturer's instructions. Spectra were collected in a 4 mL quartz cuvette with a 1 cm pathlength. The experiments were performed at 25°C in a thermostatted cuvette holder fitted with a circulating water bath. A buffer background spectrum was collected and subtracted from each sample spectra to correct for small amounts of fluorescence/scattering

from the buffer and to subtract the water Raman peak from the sample spectra. Spectra were collected within the manufacturer's recommended linear range of the instrument (1-2 million counts per second, CPS). Each sample was diluted to 50 μg/mL directly into the cuvette and was mixed by gently pipetting with a 1 mL pipetman.

2.8. Bioassay

A 96-well titer plate was coated with either non-phosphorylated or phosphorylated peptide in the presence of bovine serum albumin (BSA), washed with phosphate-buffered saline (PBS) and blocked with 1% BSA in PBS. The intact IgG1 and FITC-IgG were diluted to 2.5 μg/mL with PBS containing 1% BSA and then serially diluted 4-fold with the same buffer. These diluted samples were added to the wells and incubated at 37°C for 1 hour. The wells were then washed with PBS, and then HRP-conjugated goat anti-rabbit antibody was added for detection. The cells were washed with PBS again and developed with ultra TMB-ELISA substrate. Reaction was stopped after 5 min with 2 N H_2SO_4. The plate was read at 450 nm.

3. Results and Discussion

It is expected that the number of conjugated drugs per antibody molecule determines not only pharmacological efficacy but also spectroscopic and hydrodynamic properties of the ADCs. Thus, focus has been given to determine the ratio of the drug to the antibody and its heterogeneity using various chromatographic techniques (*13*). Here, we show below structure characterizations of ADCs using non-chromatographic techniques.

3.1. Isoelectric focusing

FITC reacts with amino groups of the antibody and hence reduces one positive charge per labeling. FITC has a negative charge which adds one negative charge per labeling. Therefore, in total, labeling one amino group results in the addition of 2 net negative charges, which should decrease the isoelectric point of the IgG. Figure 1 shows IEF analysis using a pH 3-10 gel system for the intact IgG1. Several protein bands around pH 8.3 were observed in part due to heterogeneous glycosylation. Figure 1 also shows the distribution of pI isoforms after FITC labeling. The number of stained bands greatly increased, indicating that the labeling resulted in increasing heterogeneity as expected from random labeling. The bands distributed around pH 7.0, indicating that the pI shifted to a lower pH as expected from increased net negative charges. The large shift in pI clearly demonstrates that the IgG has been labeled by FITC.
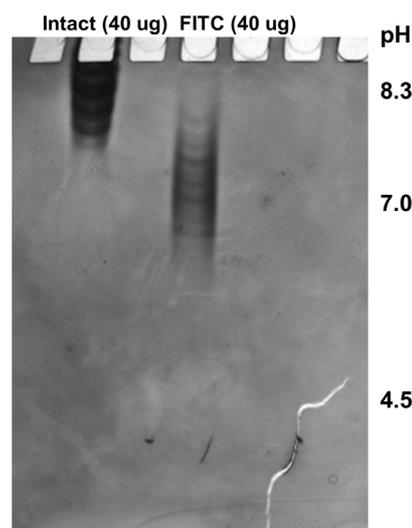

Figure 1. Isoelectric focusing. pH 3-10 gel was loaded 40 μg each of intact IgG and FITC-IgG.

3.2. Labeling ratio

FITC has absorbance in the visible region with a maximum at 491 nm and in the UV region (*e.g.*, at 280 nm) where protein absorbs. The ratio of UV absorbance at 280 nm to the value at 491 nm for FITC was determined to be 0.52 from the absorbance spectrum of free FITC. The UV absorbance spectrum of FITC-IgG showed the absorbance at 491 nm as 0.35 and at 280 nm as 0.76. Using the above ratio, the contribution of FITC absorbance at 280 nm was calculated to be 0.18, indicating the UV absorbance at 280 nm from the protein portion of FITC-IgG to be 0.58. Using the extinction coefficient of 1.4, the protein concentration was calculated to be 0.416 mg/mL. From the absorbance of 0.35 at 491 nm, the concentration of FITC in the FITC-IgG solution was calculated to be 3.13×10^{-3} mg/mL based on the absorbance of free FITC. Converting these weight concentrations to molar concentrations, the labeling ratio was determined to be 2.8 mol FITC per mol protein. Thus, labeling adds on average 5.6 net negative charges and 2.8 molecules of fluorescein per protein molecule. Such addition should also increase hydrophobic binding to both Capto MMC and Capto adhere (that were used to remove free FITC) and should decrease electrostatic binding to Capto MMC but increase electrostatic binding to Capto adhere. Since labeling is expected to increase both hydrophobic and electrostatic binding, Capto adhere may be utilized to fractionate FITC-IgG with different degrees of labeling. Although the Capto adhere chromatography used above did not show separation, a more optimal elution condition may be developed for fractionation of labeled isoforms. It is expected that higher labeling has stronger binding to Capto adhere column through enhanced hydrophobic and electrostatic interactions (when amino groups are used for conjugation).
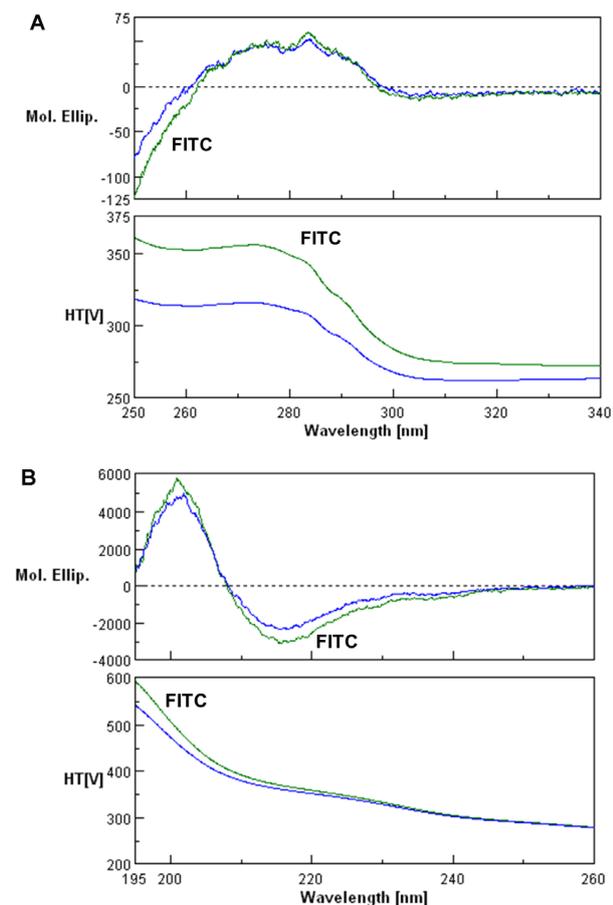
Figure 2. Near (A) and far (B) UV CD spectra. Intact IgG, blue; FITC-IgG, green.

Figure 3. Sedimentation velocity analysis of the intact and FITC-IgG antibodies. (A) Intact IgG, **(B)** FITC-IgG1. The inset shows a magnified view so that the minor peaks can be seen.

3.3. *Circular dichroism*

CD measurements were carried out at 0.416 mg/mL protein for both intact and FITC-IgG in 10 mM phosphate, pH 6.5. Figure 2A shows the near UV CD spectra (upper panel) and HT[V] spectra (lower panel) of intact IgG1 (blue) and FITC-IgG (green). The HT[V] signals closely follow the absorbance properties of the samples and are stronger for FITC-IgG1 (green), despite an identical protein concentration, reflecting that it has contribution from FITC absorbance. This difference in UV absorbance was used to determine the FITC and protein concentration of the conjugated molecule. The CD spectra, expressed as mean residue ellipticity, were nearly identical above 260 nm, indicating that FITC labeling does not alter the tertiary structure of the protein nor generate new CD signals: note that free FITC itself has no CD in this wavelength region (data not shown). It is possible that FITC conjugation to the antibody generates CD signals. Figure 2B shows the far UV CD spectra of the intact (blue) and FITC-IgG (green) in the same buffer. The HT[V] signals are slightly stronger for FITC-IgG1 in this region, consistent with the fact that free FITC has
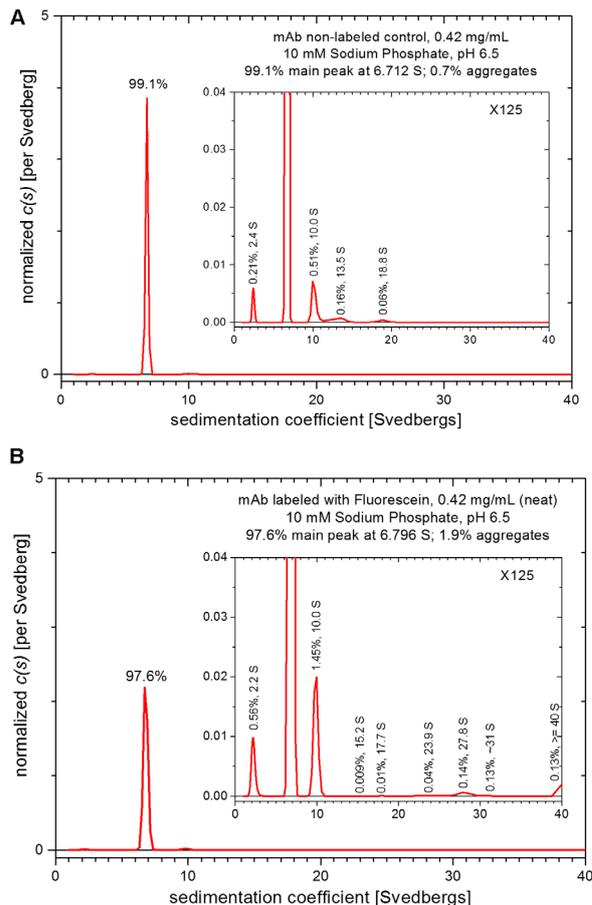
weak absorbance (data not shown). There is no far UV CD as well with free FITC (data not shown). Both spectra have a minimum at 217 nm and a maximum at 202 nm, characteristic of antibody structure. However, the CD intensity appears to be significantly stronger for the FITC-IgG, suggesting a small effect of labeling on the secondary structure of IgG.

As many cytotoxic drugs have UV absorbance that can interfere with optical properties of ADCs (*13*), this study demonstrates that care should be exercised to determine accurate protein concentration for CD analysis and then CD can be used to assess the effects of drug conjugation on the secondary and tertiary structures of the ADCs.

3.4. *Sedimentation velocity*

Figure 3 shows sedimentation velocity experiments that were carried out at 0.42 mg/mL for both the labeled FITC-IgG (green) and unlabeled IgG (blue), at 40,000 RPM and 20°C in 10 mM phosphate, pH 6.5. The raw data were analyzed by the c(s) method to obtain the size distribution. Each distribution was normalized so that the total area under the curve is

equal to 1. The FITC-IgG monomer sediments at 6.796 S while the unlabeled (intact) IgG monomer sediments at 6.712 S. The expected intra-run variability for this experiment is ± 0.006 S; thus, we are able to detect a small increase in the sedimentation coefficient upon labeling IgG with FITC. We expect the sedimentation coefficient to increase slightly since the molar mass of the labeled compound is predicted to increase by about 0.7%. However, this technique is also sensitive to changes in shape, so it is not clear from this experiment alone if this increase is due to the increase in mass or if it is due to a slight compaction of the tertiary structure, resulting is a slightly faster sedimenting molecule. Note that the near UV CD has shown unaltered tertiary structure by FITC labeling, suggesting that the slight increase in sedimentation coefficient may in fact be due to the increased molar mass of the conjugated mAb.

The unlabeled mAb control is highly homogeneous, giving 99.1% main peak. Three peaks are detected that sediment faster than the main peak, which account for 0.7% of the total sedimenting absorbance. Presumably these peaks reflect antibody aggregates and not high molecular weight impurities. A single peak is detected that sediments slower than the main peak, at 2.4 S (0.21%). The aggregate content of FITC-IgG increases to 1.9%, and many additional peaks are detected. The total aggregate content for this sample is close to the expected LOQ for this technique (which has been estimated at 1-2% for dimers of antibodies), indicating it is not possible to determine if the labeled and unlabeled antibodies truly display different aggregate levels from this single experiment. Furthermore, note that the very minor peaks observed for FITC-IgG are almost certainly pushing the limit of detection for this technique. Nevertheless, it should be emphasized that sedimentation velocity is a powerful technique to see the effects of drug conjugation on aggregation of the ADCs.

Both the labeled and unlabeled mAbs show a peak at 10.0 S, which is sedimenting about 1.5 times faster than the respective main peaks. This ratio suggests that the 10.0 S corresponds to an antibody dimer, however, without investigating the effect of concentration on the positions and relative amounts of these observed peaks, we cannot be certain if this peak corresponds to an irreversible or reversible aggregate of the main peak material.

3.5. Differential scanning calorimetry

Figure 4 shows the DSC data collected for both the labeled and unlabeled mAb, carried out at a loading concentration of 0.42 mg/mL. The heat capacity profile for the unlabeled mAb looks quite similar to what has been seen in the literature for the IgG subclass (*17*). The shoulder at about 80°C corresponds to the melting
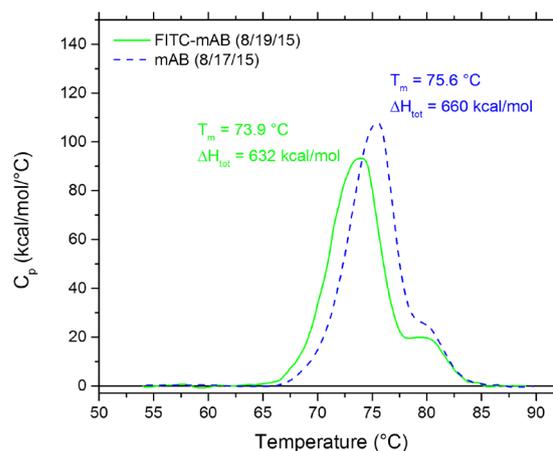

Figure 4. Differential scanning calorimetry analysis of the intact and FITC-IgG antibodies. The green trace corresponds to the FITC-IgG antibody, while the blue trace corresponds to the intact IgG antibody. The T_m values that are annotated on the graph correspond to the temperature at the maximum C_p value for the main peak. The total unfolding enthalpies (ΔH_{tot}) were calculated by numerical integration of the entire C_p curve.

of the C_{H3} region within the Fc portion of the mAb, while the rather broad peak at 75.6°C corresponds to the F_{AB} portion of the mAb. The C_{H2} region, usually seen around 70°C or so, is not obvious under these conditions, but it must be emphasized that separation of the C_{H3} profile from the F_{AB} profile is often not observed, and such separation strongly depends on the solution variables, especially pH.

The FITC-IgG shows a strong decrease of 1.7°C in the apparent T_m of the presumed FAB region, from 75.6°C (non-labeled) to 73.9°C (labeled), with no apparent difference in the C_{H3} region. This shows that the labeling of the mAb with a small, hydrophobic molecule (that only accounts for about 0.7% of the total mass) decreases the thermal stability of the molecule, and is easily detectable by DSC. While the shift in the apparent Tm is well above the expected variability for this technique (about ± 0.1°C), the apparent decrease in the total unfolding enthalpy upon labeling (4.2%) is not. The total unfolding enthalpy is dependent upon accurate knowledge of the loading concentration, which in this case carries more uncertainty than normal since it is not entirely clear how FITC affects the extinction coefficient of the protein.

3.6. Fluorescence spectroscopy

Figure 5 shows an overlay of fluorescence emission spectra collected for the non-labeled and the FITC-IgG mAbs. This experiment was conducted using an excitation wavelength of 280 nm. The peak emission wavelength was observed at 329 nm for both mAbs. This value shows that the tryptophan residues are largely buried and that labeling the mAb with FITC
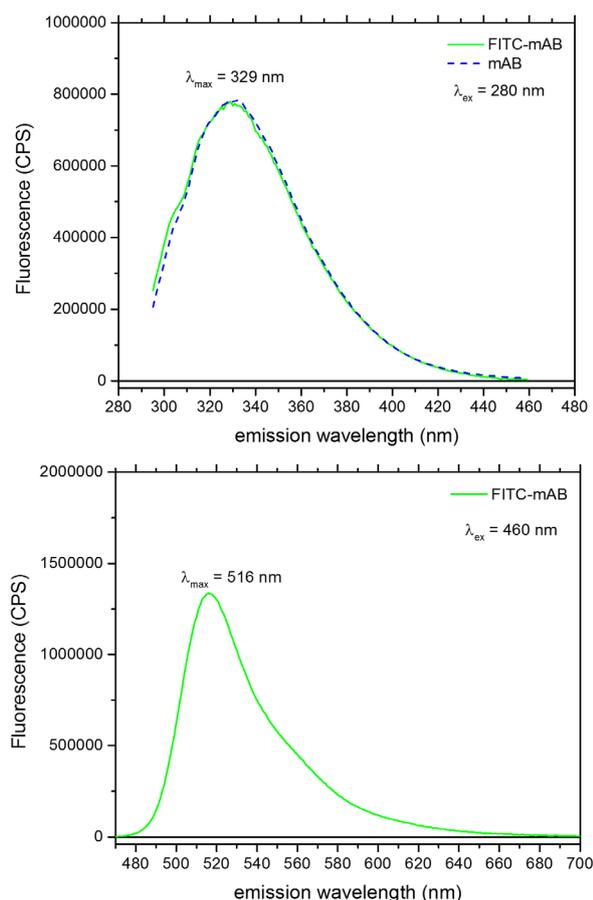
Figure 5. Fluorescence spectroscopy analysis of the intact and FITC-IgG antibodies. The green trace corresponds to the FITC-IgG antibody, while the blue trace corresponds to the intact IgG antibody. The excitation wavelength was 280 nm.

Figure 6. Bioassay of the intact and FITC-IgG antibodies.

that is characteristic of typical antibody structure in aqueous solution. Conjugation of FITC, used as a model drug in ADC, alters the secondary structure and thermal stability of the IgG, while affecting little the tertiary structure as seen by near UV CD, sedimentation velocity and fluorescence, which is consistent with unaltered biological activities. These biophysical techniques as well as separation techniques described here can be used to characterize biopharmaceutical ADC products, although it should be noted that pharmaceutical ADC contains spacer sequence between the parent antibody and the drug compound that need to be cleaved upon internalization.

does not significantly alter the environment of these tryptophan residues.

3.7. *Binding activity*

The rabbit IgG was developed to bind to a phosphorylated peptide. Binding activity and specificity were compared for the intact and labeled IgG. Figure 6 shows dose dependence of binding to a plate coated with phosphorylated and non-phosphorylated peptides. No binding of both intact IgG and FITC-IgG was observed against non-phosphorylated peptide, indicating no non-specific binding is occurring for the labeled or intact IgG molecules. Both molecules showed dose-dependent binding to phosphorylated peptide with the FITC-IgG dose curve shifted by about 3-fold to lower protein concentrations, suggesting that FITC-IgG has a slightly higher affinity for the phosphorylated peptide.

4. Conclusion

The biophysical techniques described here are routinely used to characterize pharmaceutical proteins. Characterization of the IgG antibody showed a profile
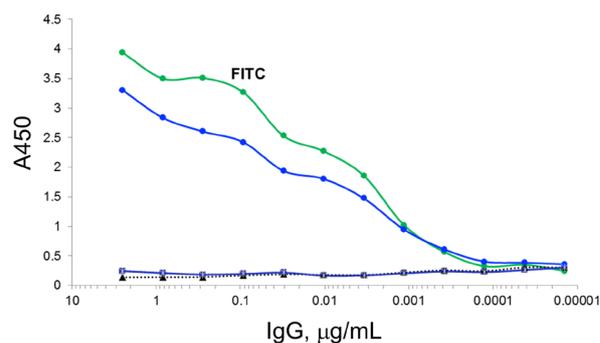
References

1. Hinman LM, Hamann PR, Wallace R, Mendez AT, Durr FE, Upeslacis J. Preparation and characterization of monoclonal antibody conjugates of the calicheamicins: A novel and potent family of antitumor antibiotics. Cancer Res. 1993; 53:3336-3342.
2. Trail PA, Bianchi AB. Monoclonal antibody drug conjugates in the treatment of cancer. Curr Opin Immunol. 1999; 11:584-588.
3. Trail PA, King HD, Dubowchik GM. Monoclonal antibody drug immunocnojugates for targeted treatment of cancer. Cancne Immunol Immunother. 2003; 52:328-337.
4. Trail PA. Antibody drug conjugates as cancer therapeutic. Antibodies. 2013; 2:113-129.
5. Weichert JP, Clark PA, Kandela IK, *et al*. Alkylphosphocholine analogs for broad-spectrum cancer imaging and therapy. Sci Transl Med. 2014; 6:240ra75.
6. Swanson KI, Clark PA, Zhang RR, Kandela IK, Farhoud M, Weichert JP, Kuo JS. Fluorescent cancer-selective alkylphosphocholine analogs for intraoperative glioma detection. Neurosurgery. 2015; 76:115-123.
7. Takahara K, Inamoto T, Minami K, Yoshikawa Y, Takai T, Ibuki N, Hirano H, Nomi H, Kawabata S, Kiyama S, Miyatake S, Kuroiwa T, Suzuki M, Kirihata M, Azuma H. The anti-proliferative effect of boron neutron capture therapy in a prostate cancer xenograft model. Plos One. 2015; 10:e0136981.
9. Li CH, Nguyen X, Narhi L, Chemmalil L, Towers E, Muzammil S, Gabrielson J, Jiang Y. Applications of circular dichroism (CD) for structural analysis of proteins: Qualification of near- and far-UV Cd for protein higher order structural analysis. J Pham Sci. 2011; 100:4642-

4654.

10. Berkowitz SA, Engen JR, Mazzeo JR, Jones GB. Analytical tools for characterizing biopharmaceuticals and the implications for biosimilars. Nat Rev Drug Discov. 2012; 11:527-540.

11. Teska BM, Li C, Winn BC, Arthur KK, Jiang Y, Gabrielson JP. Comparison of quantitative spectral similarity analysis methods for protein higher-order structure confirmation. Anal Biochem. 2013; 434:153-165.

12. Chaudhuri R, Cheng Y, Middaugh CR, Volkin DB. High-throughput biophysical analysis of protein therapeutics to examine interrelationships between aggregate formation and conformational stability. AAPS J. 2014; 16:48-64.

13. Wakankar A, Chen Y, Gokarn Y, Jacobson FS. Analytical methods for physicochemical characterization of antibody drug conjugates. MAbs. 2011; 3:161-172.

14. Arakawa T, Philo JS, Tsumoto K, Yumioka R, Ejima D. Elution of antibodies from a Protein-A column by aqueous arginine solutions. Protein Expr Purif. 2004; 36:244-248.

15. Ejima D, Yumioka R, Tsumoto K, Arakawa T. Effective elution of antibodies by arginine and arginine derivatives in affinity chromatography. Anal Biochem. 2005; 345:250-257.

16. Schuck P. Size-distribution analysis of macromolecules by sedimentation velocity ultracentrifugation and lamm equation modeling. Biophys J. 2000; 78:1606-1619.

17. Johnson CM. Differential scanning calorimetry as a tool for protein folding and stability. Arch Biochem Biophys. 2013; 531:100-109.